

Real-time small-angle synchrotron study of the crystallization kinetics of isotactic poly(1-hexadecene)

Ernesto Pérez*, Begoña Peña, and Antonio Bello

Instituto de Ciencia y Tecnología de Polímeros (CSIC), Juan de la Cierva 3,
E-28006-Madrid, Spain

Summary

The isothermal crystallization kinetics of the isotactic content of three poly(1-hexadecene) samples with different tacticity has been studied by real-time small-angle X-ray scattering using synchrotron radiation. The process was analyzed in terms of the Avrami equation. The value of the Avrami exponent was found to be approximately 1, suggesting instantaneous nucleation followed by rod-like growth. The results are compared with those previously obtained by differential scanning calorimetry.

Introduction

Crystallization of polymers is generally a nucleation-controlled process analyzed in terms of the well known Avrami equation and classical nucleation theory (1). Similar treatments have been also applied to the transformation kinetics in mesophase forming materials, both polymeric (2-8) and small molecules (9-11).

Comb-like polymers represent a special kind of macromolecules with properties distinct from those of linear and branched polymers (12). These special properties are the result of the existence of relatively long branches regularly spaced every a few atoms of the main chain. If these lateral branches are sufficiently long, a very high intramolecular ordering is developed, resulting in lateral crystallization. Polymers with long aliphatic side branches form a class of comb-like polymers exhibiting this lateral organization, similar to that obtained in n-paraffins. However, due to the presence of the main chain, only those segments exceeding about 8-10 methylene units are included in the crystal lattice (13,14). A further point which should be taken into consideration is the role of the stereochemistry in the crystallization behaviour of these polymers.

We have recently analyzed by differential scanning calorimetry, DSC, the crystallization kinetics of three poly(1-hexadecene), PHD, samples with different tacticity (15). Both the isotactic and atactic contents of the polymer are able to crystallize. However, due to problems of overlapping, only the isothermal crystallization kinetics of the isotactic polymer was studied. The results show that the process can be described by the Avrami equation up to relatively high conversions, with a rate constant which increases very rapidly

*Corresponding author

with undercooling (15), similarly to the case of mesophase forming systems.

A parallel small-angle X-ray scattering, SAXS, study on those PHD samples (15) has shown that the isotactic crystals exhibit appreciably smaller spacings than the atactic ones.

The purpose of this work is to analyze the crystallization kinetics of isotactic PHD by monitoring the corresponding diffraction in real-time SAXS experiments, using synchrotron radiation, on PHD samples isothermally crystallized from the melt. The results will be compared with those previously obtained in the calorimetric studies.

Experimental

Three samples of poly(1-hexadecene) with different isotactic content have been studied. The details of their synthesis and characterization have been reported previously (16). A $MgCl_2$ -supported $TiCl_4$ catalyst was used for the polymerization of 1-hexadecene and the different tacticities were provided by the addition of Lewis bases to the catalyst. The isotactic contents of the three samples are shown in Table 1.

Table 1.- Isotactic content of the three poly(1-hexadecene) samples determined by different methods

Sample	Isotactic content		
	DSC ^a	NMR ^a	SAXS ^b
PHD1	0.39	0.43	0.37
PHD2	0.66	0.62	0.66
PHD3	0.92	0.91	0.85

^a) Ref. 16.

^b) This work.

SAXS profiles were obtained at Daresbury Laboratory (station 8.2) using synchrotron radiation. A quadrant detector was employed at a distance of 1.6 m from the sample. The spacings covered by the experimental set-up range from about 1.5 to 35 nm. Rat-tail collagen ($L=67.0$ nm) was used for calibration.

The polymer samples were analyzed in glass capillaries of 1 mm diameter. A Linkam TMS92 temperature controller connected to a THMS600 heating/cooling stage, specially designed for capillaries, was employed. After melting the specimens at 70°C the temperature was lowered to the isothermal crystallization temperature, T_c . The scattering experiments consisted of successive time frames, each recorded over a period of 20 s. The zero time point was set to the time at which temperature equilibration was reached. The time assigned to the n th frame is then $(20n - 10)$ s. The corresponding profiles were normalized to beam intensity and corrected relative to an empty capillary background and also for the detector efficiency.

The scattering of film specimens of the three PHD samples was also analyzed at room temperature (15) with a sample-detector distance of 3.2 m (spacings ranging from about 2.7 to 60 nm).

Results and discussion

It has been shown in previous studies (15,16) that both the isotactic and atactic chains of PHD are able to crystallize, leading to structures with different melting temperatures and spacings. Figure 1 shows the melting curves of the three samples. There are two endothermic peaks, the high temperature one being attributed to the melting of the isotactic crystallites. SAXS profiles acquired at room temperature during 60 s on film samples (15) are also clearly dependent on the tacticity of the polymer (see figure 2). In fact, these curves can be fitted to two peaks, as shown by the dashed lines in figure 2. These profiles correspond to gaussian-lorentzian product functions and are centered at 0.28 ± 0.01 and $0.312 \pm 0.004 \text{ nm}^{-1}$, assigned, respectively, to the atactic and isotactic spacings. The width at half height of these peaks is also different for the two kinds of structures: 0.07 ± 0.01 and $0.045 \pm 0.005 \text{ nm}^{-1}$ for atactic and isotactic peaks, respectively. Therefore, the isotactic polymer leads to significantly thinner crystals (3.21 nm) than the atactic one (3.6 nm) and a much wider peak is obtained for the atactic chains. Therefore, these results, together with the DSC ones, suggest the presence of segregated atactic and isotactic crystallites in PHD.

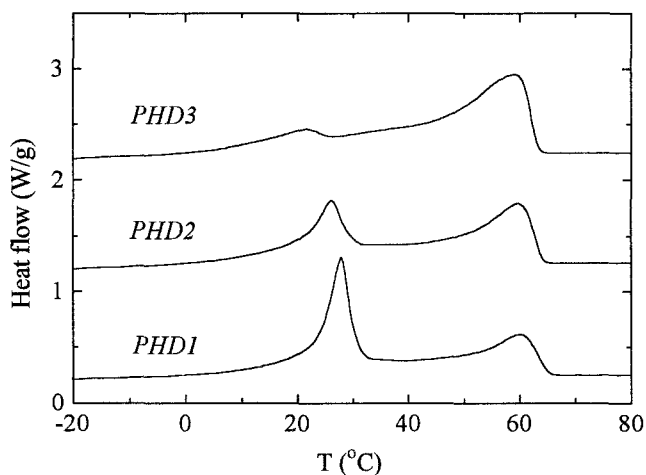


Fig. 1. DSC melting curves of the three poly(1-hexadecene) samples.

The relative areas of the two constituent peaks in figure 2 have been evaluated in order to get an independent estimation of the isotactic content in the samples. The results are

shown in the last column of Table 1. They compare fairly well with those previously obtained from DSC and NMR experiments (16), considering that the uncertainty in the fitting procedure is of the order of ± 0.005 . This agreement supports the deconvolution parameters obtained for the PHD profiles in figure 2.

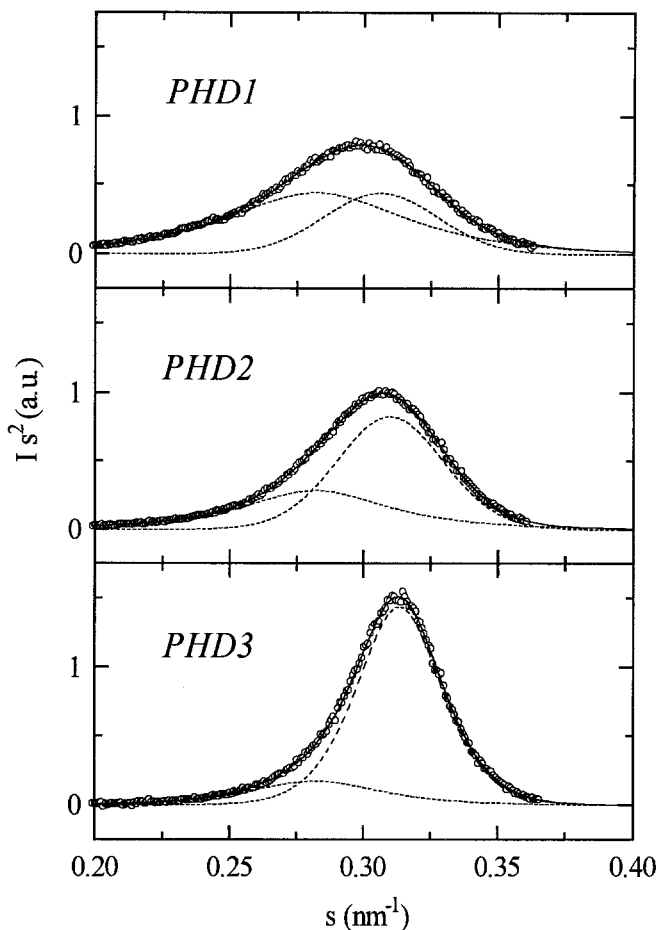


Fig. 2. Lorentz-corrected SAXS curves for the three PHD samples as a function of the scattering vector, s . The continuous lines represent the simulated profiles obtained by addition of the isotactic and atactic peaks (dashed lines).

After establishing the peak positions for both the atactic and isotactic PHD chains, the crystallization kinetics may be analyzed by SAXS if real-time conditions are used. However, it was pointed out before that, due to problems of overlapping, only the isothermal crystallization kinetics of the isotactic content can be studied.

Figure 3 shows the evolution of the isotactic SAXS peak as a function of time for a sample of PHD3 isothermally crystallized at 44.2°C from the melt. This temperature has been chosen for practical reasons: the crystallization rate is slow enough to allow the observation of the initial stages while the asymptotic limit is reached at fairly short times, suitable for synchrotron experiments.

The signal-to-noise ratio in figure 3 is appreciably worse than for the film samples, due to the smaller acquisition time. Nevertheless, these curves have been successfully fitted to a single gaussian-lorentzian product function, centered at $0.316 \pm 0.006 \text{ nm}^{-1}$. The peak center does not shift with time and corresponds very well to the isotactic position determined in the film samples. The same results have been found in the isothermal crystallization of samples PHD1 and PHD2, at temperatures of 48.2 and 49.2°C, respectively. The corresponding profiles are similar to those in figure 3 for PHD3.

From these data, the crystallization kinetics has been analyzed in terms of the Avrami equation (17-19):

$$X_c(t) = 1 - \exp(-kt^n)$$

where k is a kinetic constant of the crystallization process and the exponent n is a parameter defining the mode of nucleation and crystal growth geometry (1). The extent of the crystallization at time t , $X_c(t)$, is determined as the ratio of the area under the curve at time t to that of the final area. The representations of this equation in the usual double logarithmic plots for the three poly(1-hexadecene) samples are shown in figure 4. The values of n can be obtained from the slopes of the linear least-square fittings of the data for each sample. Considering the experimental errors, it is deduced that the Avrami exponent for the three samples is 0.9 ± 0.15 . Polymer PHD1 seems to display a smaller value of n , but it has to be considered that the errors are larger for this sample because the areas involved are smaller, due to its low isotactic content.

The value of the Avrami exponent obtained from these SAXS experiments is, therefore, close to unity, which is indicative of instantaneous nucleation with rod-like growth (4,5). This result contrasts with the value of $n=4$ obtained from DSC measurements (15), which suggest homogeneous nucleation followed by three-dimensional growth. An explanation for this discrepancy is not obvious. One possibility is that the crystallization inside thin glass capillaries, used in the SAXS experiments, proceeds from heterogeneities on the glass surface. It should be borne in mind that there is a considerable amount of material in contact with that surface. This argument may also account for the much higher

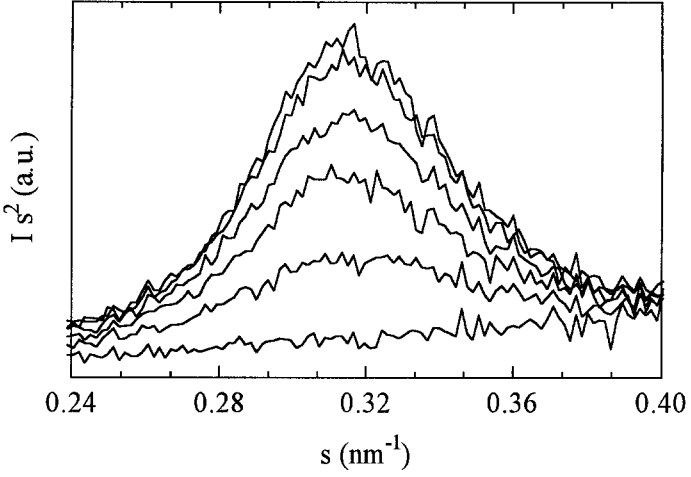


Fig. 3. Lorentz-corrected SAXS profiles, at different times, for PHD3 isothermally crystallized at 44.2°C. The curves correspond, from bottom to top, to 10, 50, 90, 150, 370 and 530 s, respectively.

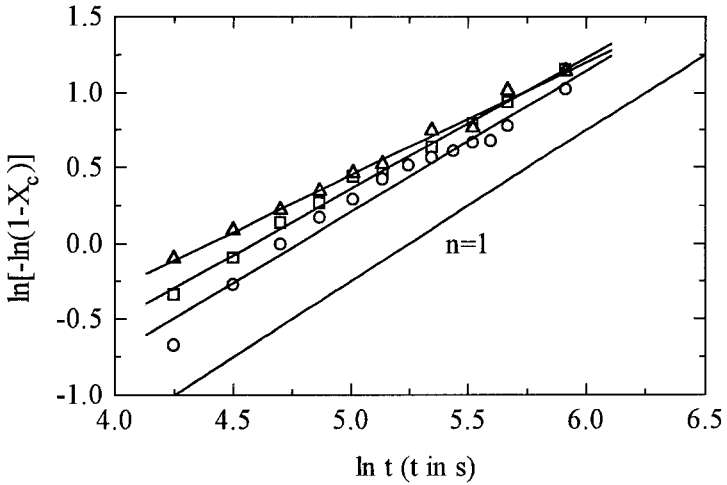


Fig. 4. Avrami plots for the three PHD samples. Δ PHD1, \square PHD2, \circ PHD3.

crystallization rate found in these experiments compared with those found by DSC (15), particularly for samples PHD1 and PHD2.

Another important aspect to consider is the final, asymptotic area obtained in the SAXS experiments. These values, in arbitrary units, are of the order of 1.4, 1.9 and 2.1 for samples PHD1, PHD2 and PHD3, respectively (increasing, as expected, with the isotactic content). However, if the samples are cooled from T_c once the asymptotic limit appears to have been reached, the peak area measured at room temperature shows a further significant increase. For instance, a value of 3.6 was obtained for PHD3. This increase is much higher than the one expected for crystallization of the atactic content, suggesting that the isotactic crystallization process was not completed at T_c .

Considering these results, a tentative explanation is the following: about two thirds of the isotactic chains (presumably the material closer to the glass surface) crystallize first through heterogeneous nucleation and one-dimensional growth at very small undercoolings. The rest of the isotactic chains (those in the interior) may experience a homogeneous nucleation with three-dimensional growth, needing greater undercoolings to proceed at appreciable rates. Unfortunately, the analysis of this second stage of crystallization of the isotactic polymer at lower temperatures is obscured by the simultaneous formation of atactic crystallites. Furthermore, the attempt to analyze these processes by optical microscopy was unsuccessful, as homeotropic structures seem to be involved in these PHD samples.

We have also observed a discrepancy in crystallization behaviour between DSC and SAXS experiments in liquid-crystalline polymers. Smectic mesophase formation from the isotropic melt in a sample of poly(heptamethylene *p,p'*-bibenzoate) exhibits an Avrami exponent of 3 in DSC experiments while we found $n=1$ in the SAXS measurements on capillary samples (20). However, the transformation of the mesophase to a three-dimensional crystal in this polymer displays an Avrami exponent of 4 in both DSC and SAXS experiments. As the 3D crystals are formed from the already partially ordered mesophase, the initial nuclei should be homogeneously distributed throughout the sample and consequently we observed no significant difference between DSC and SAXS results, in contrast to the case of mesophase development.

It has to be considered that the formation of mesophases and lateral crystallization are both very fast processes even at low undercoolings. Subtle changes on the crystallization media may have a considerable effect on the formation of the new phase.

Obviously, more experiments need to be carried out to clarify the exact cause of the changes in the Avrami exponent. Nevertheless, irrespective of the problems discussed above, the SAXS experiments presented in this work reveal that this technique is a very convenient tool for analyzing crystallization kinetics on time scales of seconds to minutes.

Acknowledgment

The financial support of the *Comisión Interministerial de Ciencia y Tecnología* (project no. MAT91-0380) and of Repsol Química S.A. is gratefully acknowledged. Dr. W.

Bras and the Daresbury Laboratory (U.K.) are also thanked for their assistance in the synchrotron experiments.

References

1. Mandelkern L (1964) *Crystallization of Polymers*. McGraw-Hill, New York
2. Warner SB, Jaffe M (1980) *J Crystal Growth* 48: 184
3. Grebowicz J, Wunderlich B (1983) *J Polym Sci Polym Phys Ed* 21: 141
4. Bhattacharya SK, Misra A, Stein RS, Lenz RW, Hahn PE (1986) *Polym Bull* 16: 465
5. Liu X, Hu S, Shi L, Xu M, Zhou Q, Duan X (1989) *Polymer* 30: 273
6. Jonsson H, Wallgren E, Hult A, Gedde UW (1990) *Macromolecules* 23: 1041
7. Cheng SZD, Zhang A, Johnson RL, Wu Z, Wu HH (1990) *Macromolecules* 23: 1196
8. Ciora RJ, Magill JH (1990) *Macromolecules* 23: 2350, 2359
9. Price FP, Wendorff JH (1971) *J Phys Chem* 75: 2839, 2849
10. Price FP, Wendorff JH (1972) *J Phys Chem* 76: 276, 2605
11. Price FP, Wendorff JH (1973) *J Phys Chem* 77: 2342
12. Platé NA, Shibaev VP (1987) *Comb-Shaped Polymers and Liquid Crystals*. Plenum, New York
13. Magagnini PL (1981) *Makromol Chem Suppl* 4: 223
14. Jordan EF, Feldeisen DW, Wrigley AN (1971) *J Polym Sci Part A* 9: 1835
15. Peña B, Delgado JA, Bello A, Pérez E (1994) *Polymer* 35: 000
16. Peña B, Delgado JA, Pérez E, Bello A (1992) *Makromol Chem Rapid Commun* 13: 447
17. Avrami M (1939) *J Chem Phys* 7: 1103
18. Avrami M (1940) *J Chem Phys* 8: 212
19. Avrami M (1941) *J Chem Phys* 9: 177
20. Pérez E, Marugán MM, Bello A, Pereña JM, unpublished results

Received: 13 June 1994/Accepted: 16 July 1994